Preparation and modification of VO_2 thin film on R-sapphire substrate by rapid thermal process*

Zhu Nai-Wei(朱乃伟), Hu Ming(胡 明)†, Xia Xiao-Xu(夏晓旭), Wei Xiao-Ying(韦晓莹), and Liang Ji-Ran(梁继然)

School of Electronics and Information Engineering, Tianjin University, Tianjin 300072, *China*

(Received 4 September 2013; revised manuscript received 24 October 2013; published online 20 February 2014)

The VO_2 thin film with high performance of metal–insulator transition (MIT) is prepared on R-sapphire substrate for the first time by magnetron sputtering with rapid thermal process (RTP). The electrical characteristic and THz transmittance of MIT in VO_2 film are studied by four-point probe method and THz time domain spectrum (THz-TDS). X-ray diffraction (XRD), X-ray photoelectron spectroscopy (XPS), atomic force microscopy (AFM), and search engine marketing (SEM) are employed to analyze the crystalline structure, valence state, surface morphology of the film. Results indicate that the properties of VO_2 film which is oxidized from the metal vanadium film in oxygen atmosphere are improved with a follow-up RTP modification in nitrogen atmosphere. The crystallization and components of VO_2 film are improved and the film becomes compact and uniform. A better phase transition performance is shown that the resistance changes nearly 3 orders of magnitude with a 2-°C hysteresis width and the THz transmittances are reduced by 64% and 60% in thermal and optical excitation respectively.

Keywords: rapid thermal process, VO_2 thin film, phase transition, modification

PACS: 81.40.Gh, 81.05.Hd, 81.40.Rs, 81.40.Tv **DOI:** 10.1088/1674-1056/23/4/048108

1. Introduction

Vanadium dioxide (VO_2) exhibits a dramatic physical behavior that a large reversible first-order change in resistivity occurs at a critical temperature of 68 °C,[1] which is referred to as metal–insulator transition (MIT) or semiconductor–metal transition (SMT).[2,3] Previous research has shown that the electrical resistivity and THz transmittance of VO_2 also have extraordinary changes during the phase transformation.[4–6] So it has been studied to apply in THz switch,[7] photoelectric switch,[8–10] phase change memory,[11,12] smart windows,[13] microbolometer,[14] and photocatalysts.[15] However, the MIT characteristics of VO_2 thin film, such as transition temperature, resistivity changing amplitude, hysteresis width, and THz transmittance vary in a wide range due to different preparation methods and substrates.[16–20] There have existed various kinds of methods of preparing the VO_2 film so far, such as vacuum evaporation,[21] reactive sputtering,[22–24] pulsed laser deposition,[25] sol–gel process,[26,27] and directed metal oxidation process (DIMOX).[20] The DIMOX with rapid thermal process (RTP) is a new method which was recently used in our laboratory to prepare vanadium oxide on silicon substrate,[28] and it has been used to prepare nano-oxide structure.[29] The advantage of this method is that the thermal oxidation and thermal annealing are combined together, and the preparation period is shortened and the controllability and repeatability are raised compared with the reactive sputtering method.[30] But silicon is a semiconductor material which is sensitive to thermal and optical excitation. The experimental results show that the performance of VO_2 thin film will be interfered with by silicon substrate. Sapphire is an appropriate substrate for epitaxial growth of VO_2 thin films. It is insensitive to thermal and optical excitation and fairly transparent to THz waves. So we select sapphire to avoid the effect of the substrate. Although much effort has been dedicated to the study on VO_2 films under different growth conditions, there are few papers dealing with the growing of VO_2 film on sapphire by DIMOX with RTP.

In this article, we use RTP to oxidize the vanadium thin film which is grown on R-sapphire substrate directly by magnetron sputtering in order to obtain VO_2 film with the properties of phase transition. In order to improve the properties of phase transition, VO_2 film is annealed in nitrogen environment by RTP again. Four-point probe method is employed to analyze the electrical characteristic of the VO_2 film, and THz-TDS is employed to analyze the THz transmittance of the VO_2 film in thermal and optical excitations.

2. Experiment

V thin film with a thickness of 70 nm is deposited on R-sapphire (1-102) substrate via direct current magnetron sputtering at ambient temperature. Two vanadium metal disks each with a high purity of 99.95% are placed face-to-face vertically as sputtered targets. The sputtering chamber is evacuated

*Project supported by the Young Scientists Fund of the National Natural Science Foundation of China (Grant No. 61101055) and the Specialized Research Fund for the Doctoral Program of Higher Education of China (Grant No. 20100032120029).

†Corresponding author. E-mail: huming@tju.edu.cn

© 2014 Chinese Physical Society and IOP Publishing Ltd

down to 2.0×10^{-4} Pa and then refilled to 2 Pa by ultra pure argon (99.99%). The total gas pressure and sputtering power are maintained at 2 Pa and 135 W during deposition, respectively.

The V thin film is annealed in a rapid thermal annealing system (AG 610) in different conditions as shown in Table 1. The VO_2 film with the best properties of phase transition is generated when it is annealed in pure oxygen atmosphere at 450 °C for 60 s (denoted as S1). In order to improve the properties of phase transition, the S1 is treated by RTP at 450 °C for 40 s in pure nitrogen atmosphere again (denoted as S2). The crystalline information of the thin film is investigated by X-ray diffraction (XRD) (D/MAX2500) with CuKα. The surface valence state and the components of vanadium are determined by x-ray photoelectron spectroscopy (XPS) (PHI-1600). The surface morphology of the thin film is observed by atomic force microscopy (AFM) (Nanosurf easyScan 2) in tapping mode and search engine marketing (SEM) (hitachi S-4800).

The electrical property of the sample is tested by a four-probe setup using a temperature controller with an accuracy of 0.1 °C. The optical property of the sample is analyzed by 8-F THz time-domain spectroscopy system. The system is located in a chamber full of dry air to avert the interference of vapor. The THz setup is based on Ti:sapphire amplifier system for intense 50-fs pulse laser with a central wavelength of 800 nm at a repetition rate of 100 MHz. The effective spectrum ranges from 0.3 THz–2.5 THz, and the average power is 520 mW. The exciting laser is from a continuous wave laser with a central wavelength of 1040 nm and a maximum power of 2000 mW.

Table 1. Phase transition characteristics of samples.

		RTP conditions	Resistance at 20° (kΩ/□)	Resistance at 80° (kΩ/□)	Resistance changing
RTP in oxygen atmosphere	Different annealing temperature	420 °C/60 s	0.2146	0.1643	1.3
		450 °C/60 s (S1)	332.5	1.882	176.9
		480 °C/60 s	660.3	59.81	11.0
	different annealing time	450 °C/40s	0.9911	0.4403	2.3
		450 °C/60 s (S1)	332.5	1.881	176.9
		450 °C/150s	437.2	25.30	17.2
RTP in nitrogen atmosphere		450°/40 s (S2)	79.12	0.1100	718.2

3. Results and discussion

Figure 1 shows the XRD patterns of S1 and S2. The patterns of S1 show peaks at $2\theta = 26.8°$, $2\theta = 37.1°$, $2\theta = 42.3°$, and $2\theta = 55.4°$ that are related to the reflection from planes (110), (200), (210), and (220) of monoclinic VO_2, respectively. This indicates that the film mainly contains several crystalline phases of monoclinic VO_2 after having been annealed in oxygen atmosphere (S1). The patterns of S2 only show a peak $2\theta = 37.1°$ which is corresponding to the reflection from plane (200) of monoclinic VO_2. So we can obtain that the crystallization of VO_2 film is improved after having been annealed in nitrogen atmosphere.

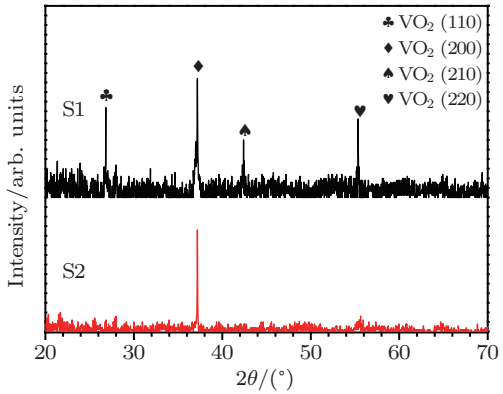


Fig. 1. (color online) XRD patterns of S1 and S2 fabricated on R-sapphire substrates.

In order to define valence state and the components more clearly, XPS is employed to examine the film. Figure 2(a) shows the XPS spectra of S1 and S2 in the O(1s), V($2p_{3/2}$), and V($2p_{1/2}$) regions. The binding energies of V($2p_{3/2}$) peak of S1 and S2 are 516.794 eV and 515.916 eV, respectively. Previous research has shown that the binding energy of V($2p_{3/2}$) peak of VO_2 is in a range of 515.7 eV–516.2 eV.[31] This illustrates that the valence state of the film becomes lower and closer to the stoichiometric value of VO_2 after having been annealed in nitrogen atmosphere. The XPS V($2p_{3/2}$) lines are fitted by Voigt lines so as to analyze the components in more detail. Figure 2(b) shows the ratios of components of S1, V^{5+} ~34.12%, V^{4+} ~44.19%, and V^{3+} ~21.69%; and figure 2(c) provides the ratios of components of S2, V^{5+} ~20.29%, V^{4+} ~50.40%, and V^{3+} ~20.29%. This suggests that V^{5+} is reduced to V^{4+} after the film has been annealed in nitrogen atmosphere.

The SEM and three-dimensional AFM patterns of S1 and S2 are depicted in Fig. 3, from which we can see that the films are composed of continuous and compact nanoparticles. The particle sizes and root-mean-square (RMS) roughness value are calculated by the image of AFM. The particle sizes of S2 (80 nm–100 nm in diameter) are much smaller than those of S1

(100 nm–200 nm in diameter), and the RMS roughness value of S2 (8.7 nm) is lower than that of S1 (11.8 nm). So we can conclude that the particle size and RMS of VO_2 film can be reduced after it has been annealed in the appropriate nitrogen atmosphere. This could be due to the fact that the crystalline phase of VO_2 film becomes more perfect in the second annealing, so the film becomes compact and uniform.

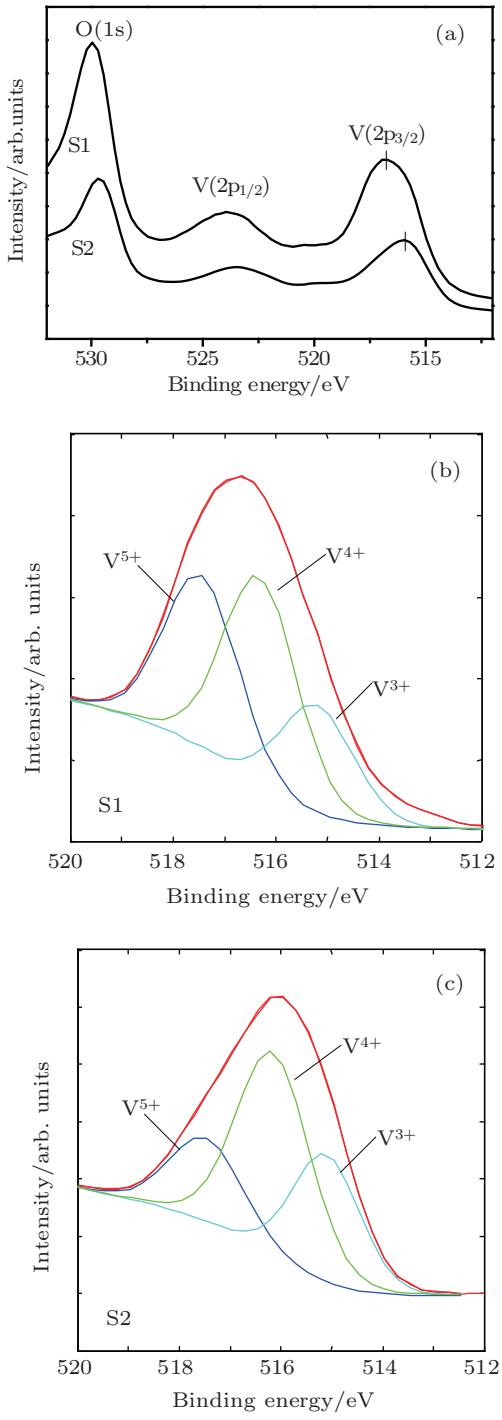


Fig. 2. (color online) XPS curves of S1 and S2 (a) $V(2p_{3/2})$, $V(2p_{1/2})$, and O(1s), (b) deconvolution of the $V(2p_{3/2})$ peaks of S1, and (c) deconvolution of the $V(2p_{3/2})$ peaks of S2.

Figure 4(a) corresponds to the temperature dependences of electrical resistivity for S1 and S2, which are measured by the four-point probe method. The abrupt changes in resistances of S1 and S2 indicate that both of the films possess excellent phase transition properties. In order to compare the phase transition characteristics precisely, we utilize the method presented by Brassard,[32] and the results are shown in Figs. 4(b) and 4(c). The transition parameters can be reflected by Gaussian fitting to the derivative of the resistance–temperature curve $(\mathrm{d}(\lg(R))/\mathrm{d}t)$. The transition temperature (T_c) is defined as the minimum value of the fitting curve; the abruptness of the phase transition (ΔT) is characterized by the full width at half maximum (FWHM) of the fitting curve; the thermal hysteresis width is defined as the difference between the heating T_c and cooling T_c. The electrical characteristics of S1 and S2 are summarized in Table 2.

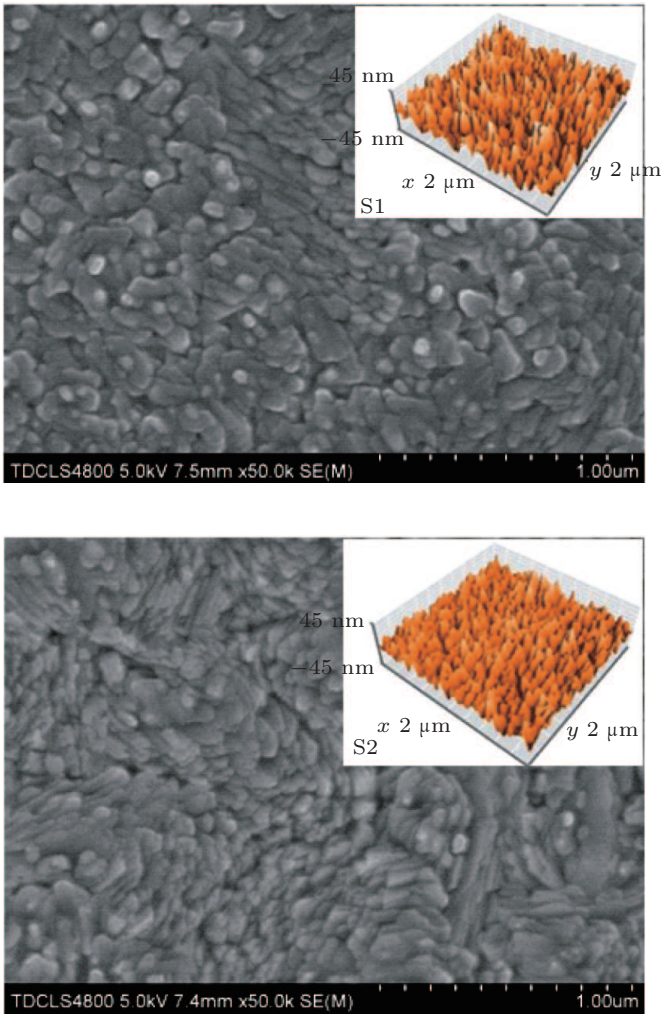


Fig. 3. (color online) SEM and three-dimensional AFM images of S1 and S2.

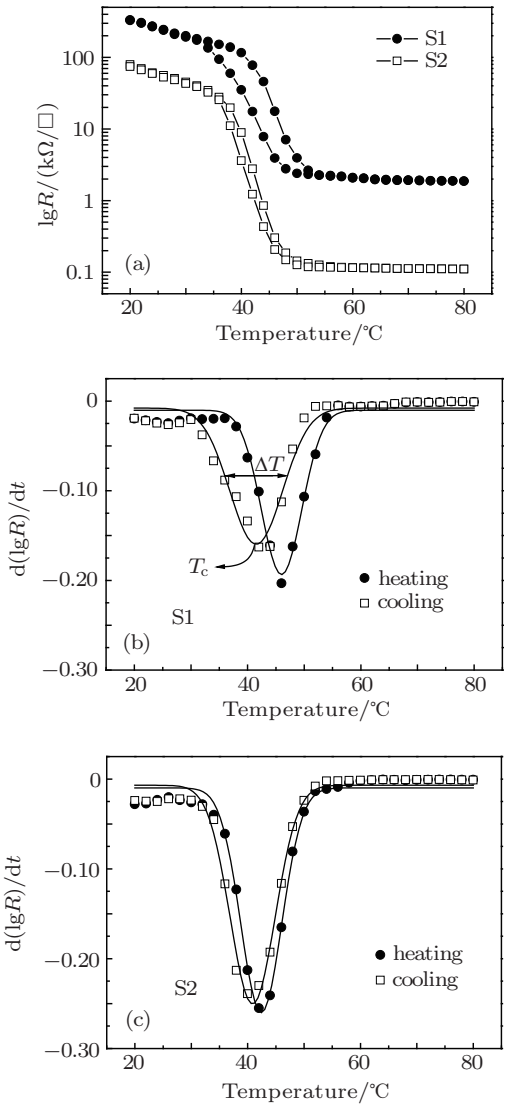


Fig. 4. (a) Resistance–temperature curves of S1 and S2, (b) Gaussian fitting of S1, (c) Gaussian fitting of S2.

Table 2. Electrical characteristics of S1 and S2.

Sample		T_c/°C	ΔT/°C	Thermal hysteresis width/°C	Resistance changing (orders of magnitude)
S1	heating	46	9	5	2.2
	cooling	41	11		
S2	heating	43	9	2	2.9
	cooling	41	11		

As can be seen from Table 2, the heating T_c of S2 is 3 °C lower than that of S1, while the cooling T_c is the same, which makes the thermal hysteresis width of S2 be 3 °C lower than S1. The values of ΔT for heating and cooling of S1 are the same as those of S2 respectively, the resistance changing of S2 is obviously higher than that of S1. It can be shown that the phase transition performance will attain a narrower thermal hysteresis and a higher resistance changing after the film has been annealed in nitrogen atmosphere. It has been reported that well-matched grains make it possible to effectively propagate the metallic regions in the films without additional energy loss, and thus narrow the hysteresis widths.[33] So the better properties of S2 in electrical characteristic may be due to the fact that the grains in VO_2 film become well-matched after the film has been annealed in nitrogen.

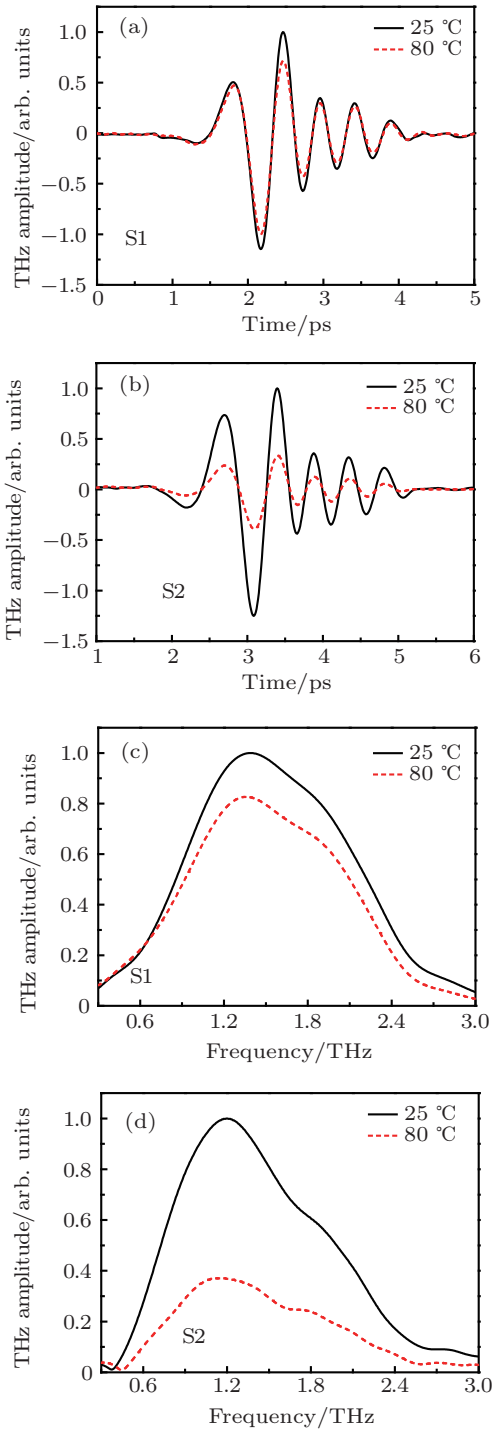


Fig. 5. (color online) Variations of THz transmission of S1 and S2 with time (a) and frequency (b) at different temperatures.

We determine the THz transmittance of the VO_2 film by THz pump–probe spectroscopy. Figures 5(a) and 5(b) show the variations of normalized time-domain THz transmissions of S1 and S2 with time at different temperatures, and figures 5(c) and 5(d) are obtained from the Fourier transforming of the time-domain data plotted in Figs. 5(a) and 5(b). Fig-

ure 6 describes the variations of THz transmissions of S1 and S2 with time at different optical excitations like the case in Fig. 5. We choose the maximum amplitude near 1.30 THz in frequency-domain curve as the reference point to compare the THz transmittance. The THz transmittances of S1 and S2 are summarized in Table 3.

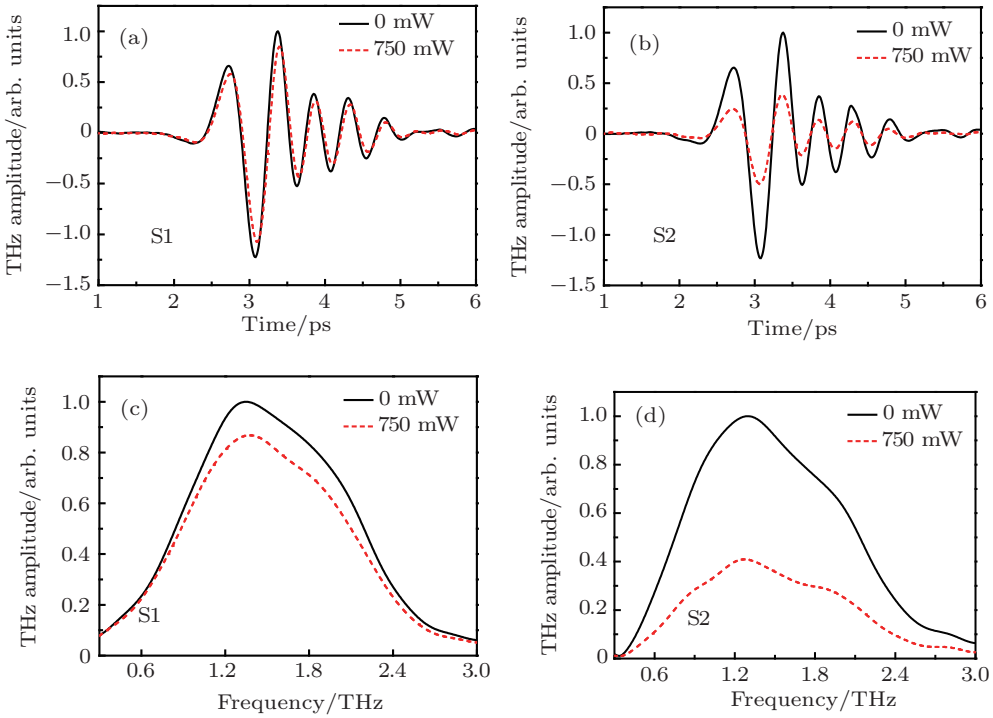


Fig. 6. (color online) Variations of THz transmission of S1 and S2 with time [(a) and (b)] frequency [(c) and (d)] at different optical excitation powers.

Table 3. THz transmittances of S1 and S2.

Sample	Thermal excitation	Optical excitation
S1	18%	14%
S2	64%	60%

Previous research has shown that the THz transmittance is influenced by the concentration of free electrons in film.[34] As can be seen from Table 3, the THz transmittance of S2 is much higher than that of S1 either in the thermal or in optical excitation. This could be due to the fact that the well-matched grains and single phase structure reduce the energy of electron transition. So S2 can energize more electrons than S1. The free electrons in S2 are enough to reflect more THz pulses so as to increase the THz transmittance of S2 significantly.

Figure 7(a) shows the temperature dependences of the normalized THz transmittance through S2, which is similar to resistance–temperature curves of S2. The THz amplitude decreases slowly before 40 °C and after 55 °C during heating, while decreases rapidly in 40 °C–55 °C. The thermal hysteresis is also observed clearly in Fig. 7(a). The laser power dependence of the normalized THz transmittance through S2 is shown in Fig. 7(b), from which we can find that the THz amplitude has no change when the laser power rises from 0 mW to 300 mW. Then the THz amplitude decreases extremely until the laser power rises to 450 mW, and finally the THz amplitude is mainly invariant.

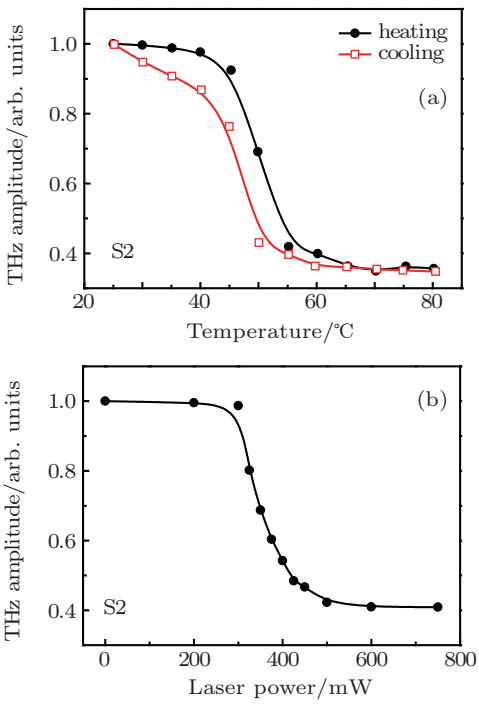


Fig. 7. (color online) (a) Temperature- and (b) laser power-dependent normalized THz transmittance through S2.

4. Conclusion

In this paper, the VO_2 thin film with high performance of MIT is prepared on R-sapphire substrate for the first time by magnetron sputtering with RTP. Vanadium film deposited on R-sapphire substrate is annealed in a pure oxygen environment by RTP to fabricate VO_2 film with phase transition properties. The film is of monoclinic VO_2 with several crystalline phases and the resistance changes 2.2 orders of magnitude during MIT. A better phase transition performance is shown after the VO_2 film has been treated by RTP at 450 °C for 40 s in pure nitrogen atmosphere. The crystallization and components of VO_2 film are improved and the film becomes compact and uniform. The sheet square resistance changes nearly 3 orders of magnitude with a 2-°C hysteresis width and the THz transmittance is reduced by 64% and 60% in thermal and optical excitation respectively.

References

[1] Morin F J 1959 *Phys. Rev. Lett.* **3** 34
[2] Ruzmetov D, Senanayake S D, Narayanamurti V and Ramanathan S 2008 *Phys. Rev. B* **77** 195442
[3] Ma J W, Xu G, Miao L, Tazawa M and Tanemura S 2011 *Jpn. J. Appl. Phys* **50** 020215
[4] Bialas H, Dillenz A, Downar H and Ziemann P 1999 *Thin Solid Films* **338** 60
[5] Pashkin A, Kubler C, Ehrke H, Lopez R, Halabica A, Haglund R F Jr, Huber R and Leitenstorfer A 2011 *Phys. Rev. B* **83** 195120
[6] Wang X J, Liu Y Y, Li D H, Feng B H, He Z W and Qi Z 2013 *Chin. Phys. B* **22** 066803
[7] Kyoung J S, Choi S B, Kim H S, Ahn Y H, Kim H T and KiM D S 2011 *AIP Adv.* **1399** 1027
[8] Soltani M, Chaker M, Haddad E and Kruzelesky R 2006 *Meas. Sci. Technol.* **17** 1052
[9] Wei X Y, Hu M, Zhang K L, Wang F and Liu K 2013 *Acta Phys. Sin.* **62** 047201 (in Chinese)
[10] Qiu D H, Wen Q Y, Yang Q H, Chen Z, Jing Y L and Zhang H W 2013 *Acta Phys. Sin.* **62** 217201 (in Chinese)
[11] Lee J S, Ortolani M and Schade U 2007 *Appl. Phys. Lett.* **91** 133509
[12] Zhang K L, Liu K, Wang F, Yi F H, Wei X Y and Zhao J S 2013 *Chin. Phys. B* **22** 217201
[13] Batista C, Ribeiro R, Carneiro J and Teixeira V 2009 *J. Nanosci. Nanotechnol.* **9** 4220
[14] Wang B, Lai J J, Zhao E J, Hu H M, Liu Q and Chen S H 2012 *Opt. Eng.* **51** 074003
[15] Wang Y Q, Zhang Z J, Zhu Y, Li Z C, Vajtai R, Ci L J and Ajayan P M 2008 *ACS Nano* **2** 1492
[16] Nag J, Payzant E A, More K L and Haglund R F 2011 *Appl. Phys. Lett.* **98** 2519161
[17] Ruzmetov D, Zawilski K T, Narayanamurti V and Ramanathan S 2007 *Appl. Phys. Lett.* **102** 113715
[18] Chen C and Fan Z Y 2009 *Appl. Phys. Lett.* **95** 262106
[19] Nagashima K, Yanagida T, Tanaka H and Kawai T 2007 *Appl. Phys. Lett.* **101** 026103
[20] Wu Z P, Yamamoto S, Miyasita A, Zhang Z J, Narumi K and Naramoto H 1998 *Journal of Physics* **10** 765
[21] Al-Kuhaili M F, Khawaja E E, Ingram D C and Durrani S M A 2004 *Thin Solid Films* **460** 30
[22] Huang Z L, Chen S H, Chen Y, Huang Y, Fu W and Lai J J 2012 *Surf. & Coat. Technol.* **207** 130
[23] Wang T, Jiang Y D, Yu H, Wu Z M and Zhao H N *Chin. Phys. B* **22** 038101
[24] Wang X J, Liang C J, Guan K P, Li D H, Nie Y X, Zhu S Q, Huang F, Zhang W W and Cheng Z W 2008 *Chin. Phys. B* **17** 3512
[25] Nakajima M, Takubo N, Hiroi Z, Ueda Y and Suemoto T 2008 *Appl. Phys. Lett.* **92** 011907
[26] Yuan N Y, Li J H and Lin C L 2002 *Acta Phys. Sin.* **51** 085205 (in Chinese)
[27] He Qiong, Xu X D, Wen E J, Jiang Y D, Ao T H, Fan T J, Huang L, Ma C Q and Sun Z Q 2013 *Acta Phys. Sin.* **62** 056082 (in Chinese)
[28] Wu B, Hu M, Hou S B, Lü Z H, Gao W and Liang J R 2012 *Acta Phys. Sin.* **61** 188101 (in Chinese)
[29] Gao W, Hu M, Hou S B, Lü Z H and Wu B 2013 *Acta Phys. Sin.* **62** 018104 (in Chinese)
[30] He L, Li Z C and Zhang Z J 2008 *Nanotechnology* **19** 155606
[31] Zhang H, Liu Y S, Liu W H, Wang B Y and Wei L 2007 *Acta Phys. Sin.* **56** 7255 (in Chinese)
[32] Alov N, Kutsko D, Spirovova I and Bastl Z 2006 *Surf. Sci.* **600** 1628
[33] Brassard D, Fourmaux S, Jean-Jacques M, Kieffer J C and El Khakani M A 2005 *Appl. Phys. Lett.* **87** 051910
[34] Chae B G, Kim H T, Yun S J, Kim B J, Lee Y W, Youn D H and Kang K Y 2006 *Electrochem. Solid State Lett.* **9** 12
[35] Jepsen P U, Fischer B M, Thoman A, Helm H, Suh J Y, Lopez R and Haglund R F 2006 *Phys. Rev. B* **74** 205103